



43871

NDB  
IN-20-TM  
COVERPAGE

NASA-TM-111435

**AIAA 95-4079**  
**Rocket-Induced Magnetohydrodynamic  
Ejector—A Single-Stage-to-Orbit  
Advanced Propulsion Concept**

J. Cole, J. Campbell, and A. Robertson  
NASA Marshall Space Flight Center  
Huntsville, AL

**AIAA 1995 Space Programs and  
Technologies Conference  
September 26-28, 1995/Huntsville, AL**

## ROCKET-INDUCED MAGNETOHYDRODYNAMIC EJECTOR—A SINGLE-STAGE-TO-ORBIT ADVANCED PROPULSION CONCEPT

John Cole, Jonathan Campbell, and Anthony Robertson  
NASA Marshall Space Flight Center  
Marshall Space Flight Center, Alabama

### Abstract

During the atmospheric boost phase of a rocket trajectory, magnetohydrodynamic (MHD) principles can be utilized to augment the thrust by several hundred percent without the input of additional energy. The concept is an MHD implementation of a thermodynamic ejector. Some ejector history is described and some test data showing the impressive thrust augmentation capabilities of thermodynamic ejectors are provided. A momentum and energy balance is used to derive the equations to predict the MHD ejector performance. Results of these equations are compared with the test data and then applied to a specific performance example.

The rocket-induced MHD ejector (RIME) engine is described and a status of the technology and availability of the engine components is provided. A top-level vehicle sizing analysis is performed by scaling existing MHD designs to the required flight vehicle levels. The vehicle can achieve orbit using conservative technology. Modest improvements are suggested using recently developed technologies, such as superconducting magnets, which can improve predicted performance well beyond those expected for current single-stage-to-orbit (SSTO) designs.

### Rocket Engine Nozzle Ejector (RENE)

For those unfamiliar with ejectors, an example that may be somewhat familiar are the ejectors used on rocket engine test stands to test altitude nozzles. At one atmosphere, the plume does not fully fill the altitude nozzle. Flow separation occurs that can damage the nozzle. The usual remedy is to place the engine inside a large tube, called an ejector, with a diameter two or three times that of the engine nozzle exit. The exhaust blows the air out of the end of the ejector at supersonic velocities, and air enters the front of the ejector at somewhat less than Mach 1. With the resulting low pressure inside the ejector, the plume fully fills the nozzle.

To assist in dispersing the flow from the ejector, a diverging section, or diffuser, is sometimes attached to the end of the ejector. When this is done, the expanding hot exhaust and air mixture frequently produces an additional thrust on the ejector of as much as 15 percent of the thrust of the rocket being tested, even when operated stoichiometrically. This additional thrust is generated without the need for any additional expenditure of fuel and is produced principally by an energy and momentum transfer to a larger accelerated mass flow. Rocket test stands are not the only place where this thrust augmentation phenomenon occurs. More than 200 papers have been written during the last several decades describing experiments and devices developed to better understand the principles involved.<sup>4</sup>

From 1962 to 1966, NASA/Marshall Space Flight Center (MSFC) was involved with the Arnold Engineering Development Center (AEDC) to determine the feasibility of using an ejector for thrust augmentation of a rocket engine.<sup>3</sup> MSFC provided the liquid oxygen/kerosene engines (lab scale versions of the Saturn V F1 engine) and part of the funding for these tests. This activity was called the RENE program and is described by several reports that were declassified in 1970.<sup>1-3</sup> During this timeframe, NASA Langley Research Center (LaRC) also performed some ejector thrust augmentation tests using a hydrogen peroxide rocket, and Marquardt built and tested several devices, initially using a monopropellant.<sup>5</sup>

The initial RENE test configuration, as shown in Fig. 1, consists of a single rocket engine placed in an ejector, with a diverging section starting at the exit plane of the engine.<sup>1</sup> The rocket engine was operated at stoichiometric conditions. Figure 2 shows the ejector assembly in the wind tunnel test cell. The wind tunnel controls the air density and flow to simulate various altitudes and Mach numbers. The tests indicated that thrust augmentations of 40 to 50 percent are possible, but that the results are sensitive to mixing efficiencies, to the ratio of secondary air flow to primary propellant flow, to the ratio of ejector length to diameter ( $L/D$ ), and to area ratios of inlet to exit.

To enhance mixing, the next set of tests used 12 engines placed around a center body tailcone as shown

Copyright© 1995 by the American Institute of Aeronautics and Astronautics, Inc. No copyright is asserted in the United States under Title 17, U.S. Code. The U.S. Government has a royalty-free license to exercise all rights under the copyright claimed herein for Governmental purposes. All other rights are reserved by the copyright owner.

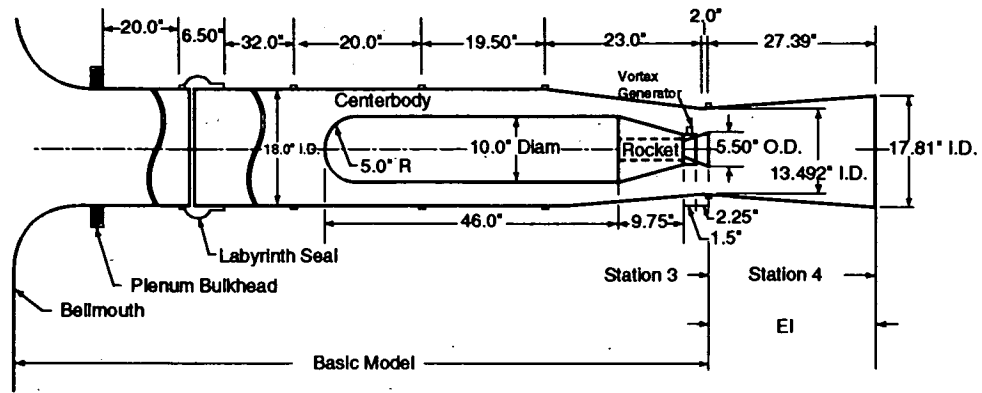


Fig. 1. Initial RENE configuration.

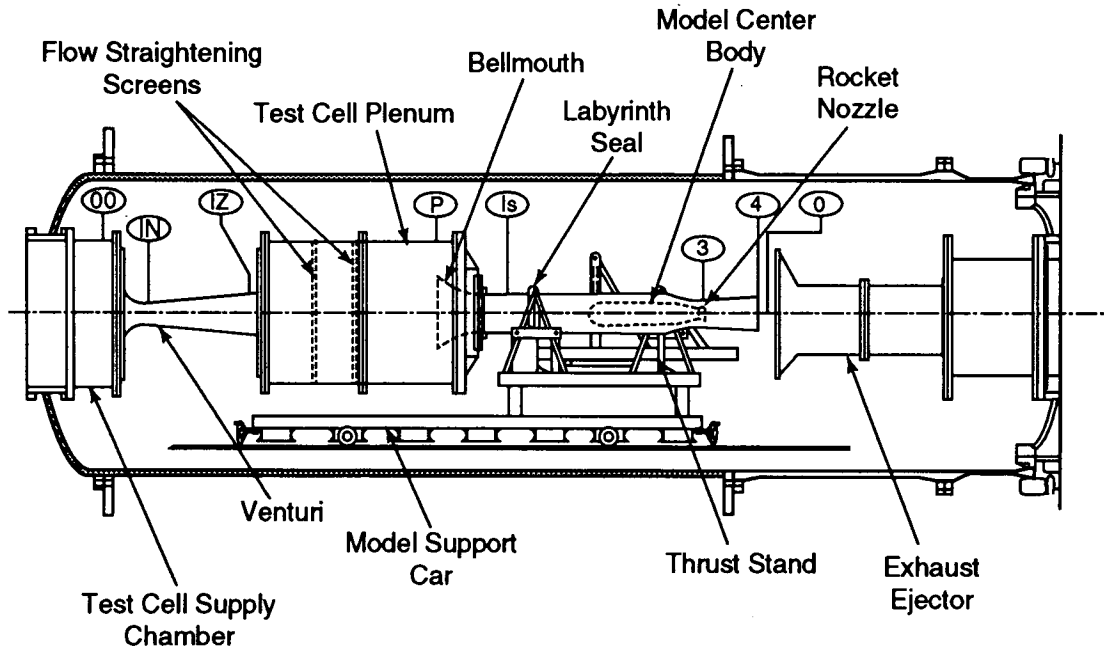


Fig. 2. Initial RENE installation in altitude test cell.

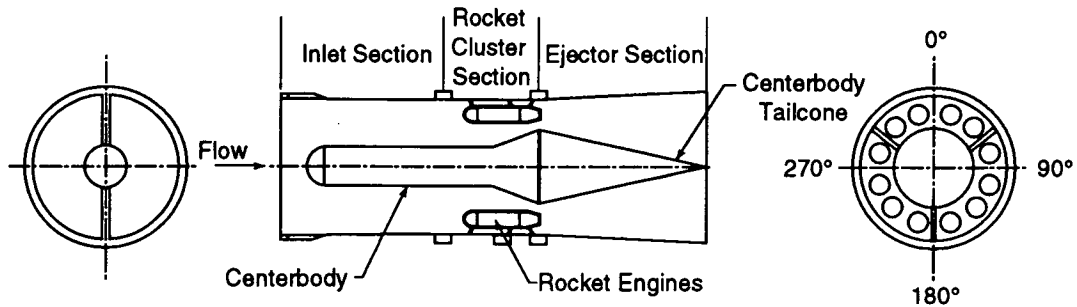


Fig. 3. Clustered RENE configuration.

in Fig. 3.<sup>2</sup> To further enhance mixing of the secondary and primary flows, small fins or vortex generators were attached around the outside of the engine bells to stir the secondary flow but not inter-

fere with the hot gas from the nozzles. Some of these mixing aids were notched or feather-cut. This assembly was placed into a test cell, and plots of some of the results are shown in Figs. 4 and 5.

Figure 4 shows that a thrust augmentation of 54 percent was obtained with a secondary-to-primary flow ratio ( $W_s/W_p$ ) of about 3.7. This case simulated performance at 40,000 ft and Mach 2.0, with ejector  $L/D = 2.0$ , and incorporating feathered-cut mixing aids. Other  $L/D$  values were not quite as efficient. However, even the worst performer, with an  $L/D = 0.6$ , succeeded in developing a thrust augmentation of 30 percent.

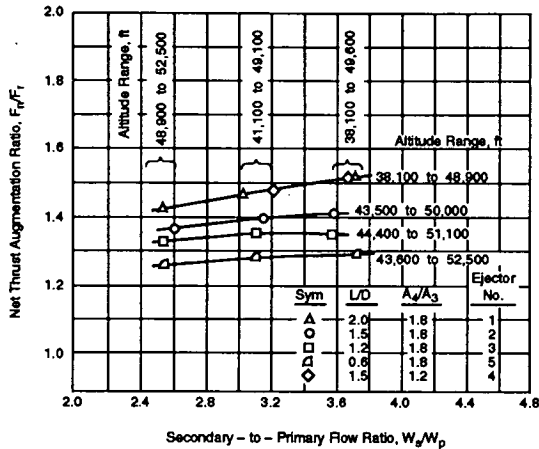


Fig. 4. RENE thrust augmentation at 40,000 ft, Mach 2, with mixing aids.

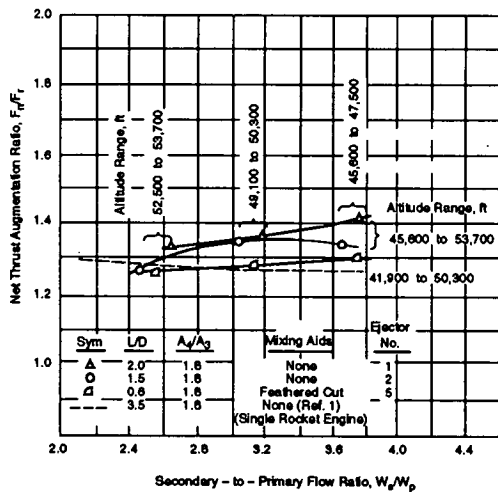


Fig. 5. RENE thrust augmentation at 40,000 ft, Mach 2, without mixing aids.

Figure 5 shows the results of essentially the same case as the previous plot except that no mixing aids were used. The  $L/D = 2.0$  still produced a thrust augmentation of about 42 percent at a  $W_s/W_p = 3.7$ . An interesting peculiarity occurs using the ejector with an  $L/D = 1.5$ ; the plot indicates a drop-off in augmentation with  $W_s/W_p > 3.2$ . A similar curve is shown in the previous Mach 2 case, but with an  $L/D = 1.2$ . This peculiarity is not addressed in the text of

the reports. The curves with best performance do not indicate any similar drop-off and, in fact, indicate that additional performance augmentation would probably be obtained at higher  $W_s/W_p$  ratios.

The results of subsonic performance at 15,000 ft and Mach 0.9 were determined. Without mixing aids, the previous best performer was only about 7 percent. With mixing aids, a thrust augmentation of 44 percent was obtained; however, the optimum  $L/D$  value changed to 1.5 and with lower area ratios. The previous best performing  $L/D = 2.0$  (for the Mach 2.0 cases) only provided 5-percent augmentation at this subsonic condition. This indicates that geometric articulation of the ejector length and area ratios is required between subsonic, supersonic, and hypersonic velocities. Marquardt Corp. studies indicate that this effect may be achievable with a secondary injection of fuel at points that differ with velocity; specifically, near the ejector exit at lift-off and forward of the primary rockets when above Mach 4.<sup>5</sup>

Figure 6 has a different x-axis but shows that operating the rockets in a fuel rich mode (all the previous runs were stoichiometric) at  $W_s/W_p = 5.0$  produced thrust augmentations by a factor of 2.4 or by an additional 140 percent.<sup>3</sup> This additional performance is attributed to combustion of the extra fuel with the oxygen in the secondary flow. The results are impressive. However, in 1967, funds for this activity ran out and the project was concluded.

The rocket-based combined cycle (RBCC) engine concept, currently being pursued by Bill Esher at NASA-Headquarters, utilizes both the ejector mode and secondary fuel injection to augment thrust.<sup>6</sup> Aerojet has developed an RBCC concept called a strutjet which is currently being tested at both LaRC and NASA Lewis Research Center (LeRC).<sup>7</sup>

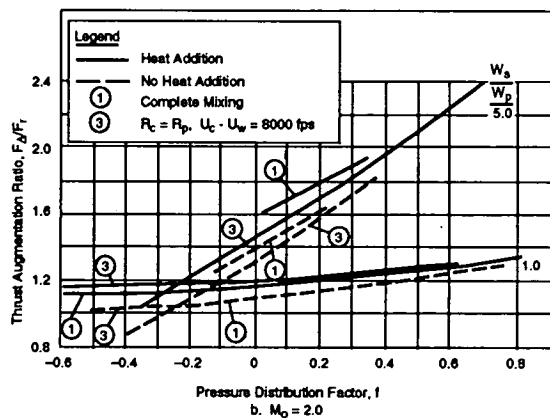


Fig. 6. RENE thrust augmentation, Mach 2, effect of heat addition.

## Other Ejector Experience

During the RENE timeframe, many other laboratories and institutions were investigating ejector thrust augmentation.<sup>4</sup> Figure 7 shows the test results from 25 investigations and indicates that many of them obtained greater than 50 percent thrust augmentation, several by a factor of 2.5.

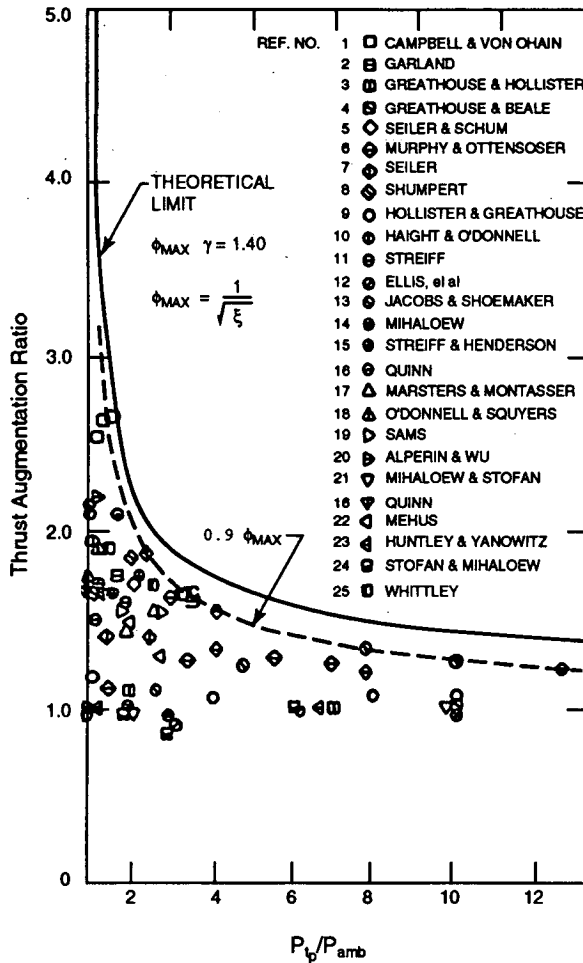


Fig. 7. Other ejector research.

A consistent observation from all is that the geometry for optimum performance depends strongly on the Mach number and dynamic pressure level. Cruise vehicles may be able to exploit a fixed geometry once they obtain cruise conditions. Accelerator vehicles, however, such as those going into space, must be able to articulate the geometry to remain near the optimum performance. Many articulated geometry concepts have been examined to permit operation over the ranges needed to accelerate a vehicle toward space. Typically, these concepts are quite complex and weigh an order of magnitude more than the rocket engine alone. This complexity and large engine mass has been largely responsible for the

lack of significant implementation of this principle in the United States. The French and the Russians have several fixed geometry missile applications utilizing ejectors or ducted rockets. Aerojet is testing a clever RBCC concept called a strutjet that reduces complexity, weight, and development costs.<sup>7</sup>

Another observation is that the performance continues to improve with increased bypass ratio. Theoretically, performance increases with the square root of the bypass ratio, but thermodynamic laws constrain the practical limits for taking advantage of this square root relationship. When the velocity of the secondary flow equals the velocity of the primary flow, there can be no further kinetic transfer of energy and momentum regardless of the bypass. Also, since this exchange of energy and momentum requires a finite amount of time, higher secondary flow velocities require longer ducts to accomplish the mixing. Because of the large size and mass of high bypass ducts, bypass ratios larger than 5 are difficult to implement.

However, thermodynamics is not the only mechanism available to engineers for designing an ejector. Exchange of energy and momentum can also be accomplished electromagnetically using the principles of MHD. Advantages for considering MHD include the possibilities for designs that are independent of the secondary flow velocity, that utilize the almost instantaneous energy transfer, and that permit bypass ratios significantly larger than 5, perhaps as large as 50. The disadvantages include the extremely high electrical power involved (about a gigawatt) and the heavy mass of the MHD systems if conventional MHD designs are used.

## Ejector Thrust Augmentation Principles

The benefits of using bypassing air for augmenting the thrust and performance of a rocket can be shown from a momentum and energy balance following the usual derivation of the ideal rocket equation except for adding an air bypass. These same relations show the effects of various inefficiencies in the system.

### Momentum Balance

From Fig. 8, at time  $t$  the system consists of the rocket of mass  $m$  moving at velocity  $v$  and an amount of bypassing air with which the rocket will interact. For simplification, the effects of drag, friction, shocks, and gravity will not be considered. This bypassing air with mass  $m_a$  may be moving at some velocity  $v_a$ , which may be zero. Now, at time  $t+\Delta t$ , a quantity of propellant with mass  $\Delta m$  has been ejected from the rocket. This quantity of propellant

is moving with a velocity  $v - c_p$  where  $c_p$  is the characteristic velocity of the exhausted propellant. If a part of the rocket energy is diverted from the rocket exhaust and used to accelerate the quantity of bypassing air then two effects result. First,  $c_p$  is reduced and second, the bypassing air velocity is changed to  $v_a - c_a$  where  $c_a$  is the characteristic velocity of the air from the acceleration mechanism.

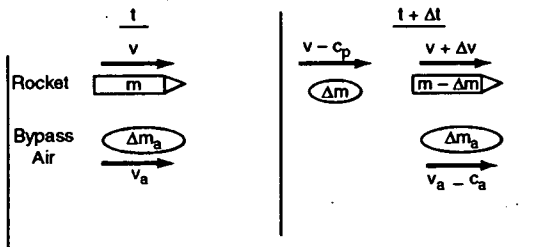


Fig. 8. Conservation of momentum, with bypass air.

Schmidt has derived the thrust augmentation relationship where the momentum exchange is a function of the difference between the propellant characteristic velocity and the velocity of the bypassing air. This formulation is more accurate for thermodynamic ejectors and ducted rockets because the momentum exchange depends on this difference. Since this paper is focused toward an MHD concept, the momentum exchange is electromagnetic and will accelerate the air flow even if it is moving faster than the rocket exhaust.

From Fig. 10, a momentum balance can be constructed as

$$mv + v_a \Delta m_a = \Delta m(v - c_p) + (m - \Delta m)(v + \Delta v) + \Delta m_a(v_a - c_a),$$

so that,

$$\Delta m c_p = m \Delta v - \Delta m_a c_a.$$

Divide by  $\Delta t$ ,

$$m a = c_p \dot{m} + c_a \dot{m}_a.$$

Expressions for  $c_p$  and  $c_a$  will be developed from an energy balance in the next section.

Now,

$$F = ma = m \dot{v}.$$

Let,

$$B = \dot{m}_a / \dot{m}, \quad (1)$$

the mass bypass ratio.

So, the augmented thrust  $F$  can be written as

$$F = (c_p + c_a B) \dot{m}, \quad (2)$$

and the augmented specific impulse  $I_{sp}$  as

$$I_{sp} = F / \dot{m} = (c_p + c_a B). \quad (3)$$

Performance augmentation can be estimated by following the derivation of the ideal rocket equation to find the burn-out velocity produced by consuming an amount of propellant established by a mass fraction  $f$ . Thus, from equation (2)

$$a = \dot{v} = (c_p + c_a B) \dot{m} / m. \quad (4)$$

Multiply by  $dt$ , and integrate  $dv$  from  $v_0$  to  $v$ , and  $dm/m$  from  $m_0$  to  $m$ ,

$$v - v_0 = (c_p + c_a B) \ln(m/m_0),$$

but

$$m = m_0 - \dot{m} t,$$

$$v = v_0 + (c_p + c_a B) \ln(1 - \dot{m} t / m_0).$$

Now, define  $f = m_p / m_0$ , the mass fraction, where  $m_p$  is the total propellant mass. The maximum velocity  $v_{max}$  will occur when  $\dot{m} t = m_p$ , when all propellant is consumed, so,

$$v_{max} = v_0 + (c_p + c_a B) \ln(1 - f).$$

If the staging velocity at burnout is defined as  $v_s = v_{max} - v_0$ , then,

$$v_s = (c_p + c_a B) \ln(1 - f). \quad (5)$$

This equation represents the augmented performance of an air bypass mechanism as determined from the ideal rocket equation procedure.

Equation (5) can be split into two equations describing the contribution to staging velocity from the residual propellant thrust, and the contribution from the bypass air. Thus,

$$v_{sp} = c_p \ln(1 - f),$$

and,

$$v_{sa} = c_a B \ln(1 - f).$$

The performance gain  $G$  can be described by

$$G = \frac{v_{sB}}{v_{sR}} = \frac{(c_p + c_a B) \ln(1-f_B)}{c \ln(1-f_R)} \quad (6)$$

where

$v_{sB}$  = staging velocity with bypass mechanism

$v_{sR}$  = staging velocity with rocket only

$f_R$  = propellant mass fraction for rocket vehicle with no bypass

$f_B$  = mass fraction adjusted to include weight of bypass mechanism.

If,

$m_{VR}$  = dry mass of the rocket vehicle with no bypass mechanism,

and

$m_{BM}$  = mass of the bypass mechanism,

then,

$$f_B = \frac{m_p}{m_{VR} + m_p + m_{BM}} = f_R \left\{ \frac{1}{1 + (m_{BM}/(m_{VR} + m_p))} \right\} \quad (7)$$

### Energy Balance

The kinetic energy of the exhaust of a rocket engine is determined by the enthalpy of the propellant and the efficiency of the engine combustion process in converting the hot gases into a high velocity flow. This energy relationship can be written as:

$$\frac{1}{2} m_p c^2 = \eta_p J H \quad (8)$$

where

$m_p$  = the mass of the propellant

$c$  = the engine characteristic velocity as defined by the above equation

$\eta_p$  = the efficiency of the engine process

$H$  = the enthalpy of the propellant

$J$  = the mechanical equivalent of heat.

Thus,

$$c = \sqrt{2\eta_p J H / m_p} \quad (9)$$

This represents the characteristic velocity of the exhaust gasses from the basic rocket engine alone.

Now, from Fig. 9, the rocket engine exhaust traveling at a characteristic velocity  $c$  passes through a bypass mechanism which extracts some energy from the flow. After some efficiency losses this diverted energy is used to accelerate part of the bypassing air.

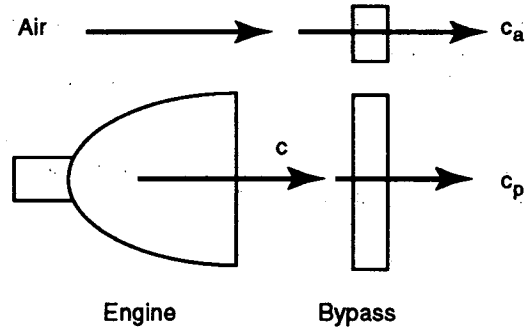


Fig. 9. Conservation of energy, with bypass air.

The energy balance can be represented by partitioning the enthalpy.

$$H_{\text{propellant}} = H_{\text{combustion loss}} + H_{\text{residual exhaust velocity}} + H_{\text{lost in bypass}} + H_{\text{lost in air coupling}} + H_{\text{air velocity increase}}$$

Define:

$R_b$  = ratio of energy diverted from the engine exhaust

$\eta_b$  = efficiency of diverting exhaust energy into the bypass mechanism

$\eta_a$  = efficiency of coupling the bypassed energy into the air stream.

Expressing each term of the partition yields

$$H = (1-\eta_p)H + \eta_p(1-R_b)H + \eta_p R_b(1-\eta_b)H + \eta_p R_b \eta_b(1-\eta_a)H + \eta_p R_b \eta_b \eta_a H \quad (10)$$

Factoring into a nested form

$$H = H[(1-\eta_p) + \eta_p[(1-R_b) + R_b[(1-\eta_b) + \eta_b[(1-\eta_a) + \eta_a]]]] \quad (11)$$

shows that each nest reduces to " = 1".

The two terms of interest are the residual exhaust velocity and the air velocity increase. The same form of the energy equation (8) can now be used to represent the characteristic velocities of the residual thrust from the rocket exhaust  $c_p$  and the accelerated bypassing air  $c_a$ . Thus,

$$\frac{1}{2} m_p c_p^2 = \eta_p(1-R_b)JH \quad (12)$$

propellant residual energy, and,

$$\frac{1}{2} m_a c_a^2 = \eta_p R_b \eta_b \eta_a J H , \quad (13)$$

energy coupled into the bypassing air, so that,

$$c_p = \sqrt{(2\eta_p J H / m_p)(1-R_b)} , \quad (14)$$

and,

$$c_a = \sqrt{(2\eta_p J H / m_p)[R_b \eta_b \eta_a (m_p / m_a)]} . \quad (15)$$

Or, using equation (9) for  $c$  and equation (1)

$$B = \dot{m}_a / \dot{m}_p = m_a / m_p ,$$

then,

$$c_p = c \sqrt{1-R_b} , \quad (16)$$

and,

$$c_a = c \sqrt{R_b \eta_b \eta_a (1/B)} , \quad (17)$$

so that the  $I_{sp}$  from equation (3) can now be written as

$$I_{sp} = (c_p + c_a B) = c \{ \sqrt{1-R_b} + \sqrt{R_b \eta_b \eta_a B} \} , \quad (18)$$

and thrust from equation (2) as

$$F = I_{sp} \dot{m} = \dot{m} c \{ \sqrt{1-R_b} + \sqrt{R_b \eta_b \eta_a B} \} . \quad (19)$$

To understand the meaning of equation (18), consider the extreme cases. If the efficiencies  $\eta_b \eta_a$  are 100 percent (i.e.,  $\eta_b = \eta_a = 1.0$ ) and if 100 percent of the energy is diverted into the air flow (i.e.,  $R_b = 1.0$ ), then the  $I_{sp}$  augmentation is proportional to the square root of the bypass ratio  $B$ . Likewise, if no energy is bypassed (i.e.,  $R_b = 0$ ), then  $I_{sp} = c$ , which is the familiar definition.

Equations (16), (17), and (18) can now be substituted into equations (5) and (6) for augmented performance and gain.

An interesting observation is found when the  $I_{sp}$  in equation (18) is substituted into the gain, equation (6). The characteristic velocity  $c$  cancels out. This means that the gain is independent of the specific impulse. Gain, however, is a function of the mass fractions  $f_B$  and  $f_R$ , and the gain is a function of the square root of the bypass ratio  $B$ , a significant and important observation. Performance in equation (5) is, of course, a strong function of specific impulse.

An optimum value of  $R_b$  can be found by setting to zero the derivative of  $F$ , equation (19).

$$0 = \frac{dF}{dR_b} = \dot{m} c \frac{d}{dR_b} [(1-R_b)^{\frac{1}{2}} + (R_b \eta_b \eta_a B)^{\frac{1}{2}}]$$

or,

$$R_b = \eta_b \eta_a B / (1 + \eta_b \eta_a B) , \quad (20)$$

for maximum thrust  $F$ .

To understand the significance of equation (20), assign a set of values to the product

$$\eta_b \eta_a B = (0, 1, 2, 3)$$

which yields

$$R_b = (0, 1/2, 2/3, 3/4) .$$

This shows that the optimum energy bypassed from the rocket is such that all the propulsive mass, including both the propellant and bypass air, shares the energy equally. Thus, if the efficiencies were 100 percent, then when the bypass air mass is equal to the propellant,  $B = 1$ , half the optimum bypass energy is diverted into the air and half remains with the propellant. When  $B = 3$ , then 3 parts of the energy should go into the air and 1 part should remain with the propellant. The efficiency factors, of course, reduce the total amount of energy available to be divided, and thus the amount that should be diverted. For very large bypass ratios the message is that the maximum energy possible should be diverted into the bypass flow for as long as the bypass flow is available.

### Theoretical Potential of MHD Ejectors

Equations (5), (16), and (17) calculate the stage burnout velocity when all the propellant is consumed as defined by the mass fraction  $f$ .  $R_b$  is the percentage of the rocket energy that is diverted from the rocket, some of which is eventually transferred into the bypassing air. A coupling efficiency,  $e = \eta_b \eta_a$ , is included that accounts for the fraction of the diverted energy lost during the conversion processes and not delivered to the bypassing air.

Fig. 10 shows the results of stage burnout velocity plotted against the fraction of the rocket energy diverted into the bypassing air, for a family of bypass ratios and for  $f = 0.67$ ,  $I_{sp} = 425$  s, and  $e = 0.49$ . The very poor mass fraction  $f$  is to account for the high mass of the MHD hardware based on current designs, as will be explained. Similarly, the compromised  $I_{sp}$  is for expected average performance between sea level and vacuum. The extremely low efficiency  $e$  reflects no energy recovery techniques.



These conservative assumptions can, no doubt, be improved with a careful system design and by using recent technologies, such as superconducting magnets.

With this poor design, the zero bypass point is only able to achieve a burnout velocity of 4,500 m/s, while 10,000 m/s is usually considered to be the required ideal velocity to reach orbit, when the effects of drag and gravity losses are added in. The case for a bypass ratio of  $B = 3$  matches the results of the RENE project by providing 50 percent of performance augmentation. Without mixing aids, the RENE data show only 40-percent augmentation. This indicates a low-energy transfer, perhaps  $R_b = 0.2$ , and the graph indicates about 40-percent augmentation for this case. For this design,  $B = 3$  achieves 7,200 m/s, much less than that required to obtain orbit.  $B = 10$  exceeds the 10,000 m/s orbit requirement, but the drawback is that bypass air is not available all the way to orbit. Most rocket trajectories leave the atmosphere before achieving half the delta velocity needed for orbit. The remaining delta velocity must be obtained by rockets alone. For the later vehicle sizing analysis, a bypass ratio of  $B = 30$  has been selected and should just achieve orbit with the poor design parameters described above. Even minor design improvements will increase performance significantly. Some avenues for such improvements will be suggested later.

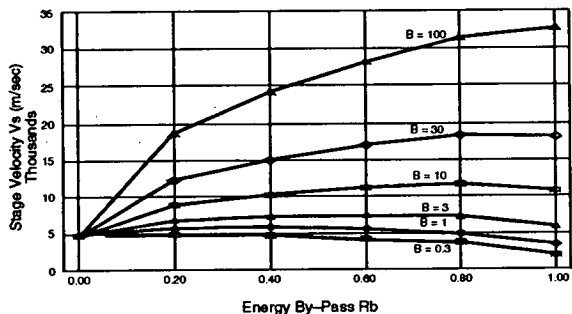


Fig. 10. Ideal ejector performance.

### The MHD Concept

The RIME engine (Fig. 11) has four components: the rocket engine, MHD generator, ionizer, and MHD accelerator. The rocket engine is the energy source for the entire system and is fueled by liquid hydrogen and liquid oxygen carried in tanks within the vehicle. It provides a very high velocity flow of ionized gas.

A thermodynamic ejector transfers energy and momentum from the rocket exhaust into the bypassing air flow. Likewise, the MHD ejector first extracts electrical energy from the rocket exhaust using an MHD generator (Fig. 12). Hot ionized gas flows through a magnetic field  $B$  (not to be confused with the bypass ratio symbol, also expressed as  $B$ ). The Lorentz  $B \times v$  force on the ions and electrons pushes the electrons toward one electrode and the ions toward the other, creating an electrical potential across the electrodes. Thus, electric current can be generated at the expense of kinetic energy in the gas flow. This electric current can be used to supply power to the generator magnets, to the ionizer, and to the accelerator. One can readily show that a 150,000-lb-thrust rocket engine at 80-percent efficiency can generate 1.0 gigawatts of electrical power.

Cold bypassing air does not contain ions in adequate quantities to be useful in an accelerator. An ionizer is, therefore, needed to increase the air conductivity to adequate levels.

The MHD accelerator is designed and operates similarly to the MHD generator, except that a high potential is imposed on the electrodes in opposition to the  $B \times v$  force which will accelerate both the ions and electrons in the direction of the velocity of the flow. The entire gas does not need to be ionized. If the gas contains 1-percent ions, then the entire gas can be accelerated through collisions between the ions and other gas molecules.

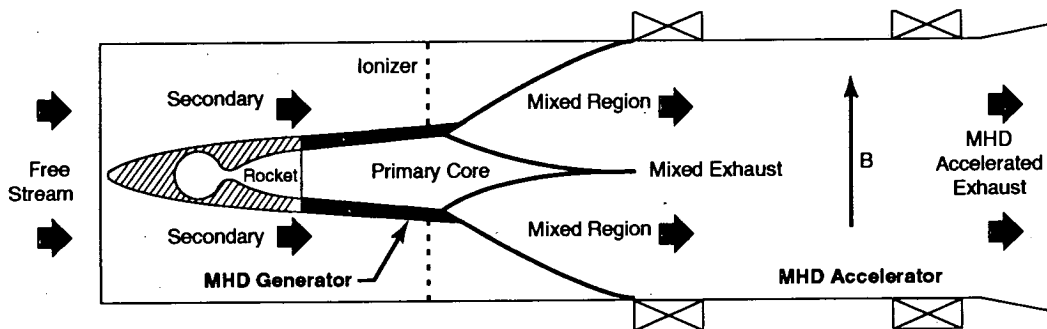


Fig. 11. RIME engine concept.

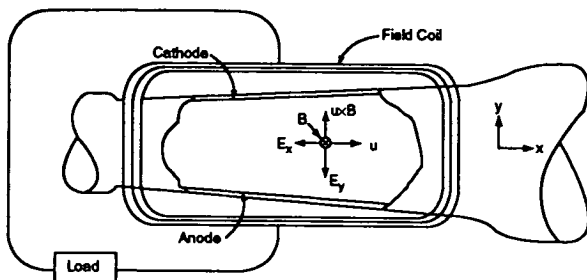


Fig. 12. MHD generator.

The RIME concept shown in Fig. 11 is arranged to resemble a thermodynamic ejector. Other arrangements may improve efficiency. If the bypass ratio is large, there will be little benefit in mixing the exhaust with the bypass air, except perhaps for the ionization benefits. A configuration which would eliminate the ducts for bypassing air, saving mass and reducing drag, is to utilize external electric and magnetic fields as shown in Fig. 14. This concept, in effect, utilizes the skin of the vehicle as the MHD accelerator, an inside-out accelerator. Examples of such devices are not known.

#### RIME Component Technology Status

Many MHD generators have been built and operated.<sup>8</sup> AEDC has built and operated a 35-MW generator that functioned at 80 percent efficiency.<sup>12</sup> STD, Inc., built a lightweight 5-MW system for the Air Force that was installed on a flatbed trailer towed by a pickup truck.<sup>9,11</sup> STD, Inc. scaled up this design for a 100-MW version for SDI, but no hardware was built.<sup>10</sup> This design provided the data used in the RIME vehicle sizing analysis discussed later.

Ionizers can be designed using one or a combination of the following: arc jets, small auxiliary rockets, high voltage, sparks, induction, lasers, microwaves, interacting shocks, and seeding.<sup>14</sup> The simplest to implement is probably potassium carbonate seeding with a small auxiliary rocket engine. There may, however, be environmental constraints for an operational concept using this technique. Power levels required to achieve the necessary conductivity have not yet been calculated.

Several MHD accelerators have been built for use as wind tunnels. AEDC built two 35-MW MHD-driven wind tunnels that accelerate air seeded with 2-percent potassium carbonate to Mach 20.<sup>12,13</sup> One of these tunnels is a continuous flow, low-density tunnel called LORHO (from "rho,"

the Greek symbol for density) and a high-density shock tunnel called HIRHO. Conceptual designs for larger, unseeded wind tunnels have been proposed.<sup>14,18</sup> Small MHD accelerators at the kilowatt level have been proposed, built, and tested in the laboratory, and the Russians have flown small attitude control MHD thrusters.<sup>15</sup>

Other applicable technologies have been recently developed by SDI, SSC, and EPRI including superconducting magnets and high-power dc switches.<sup>15,16</sup>

Thus, all of the basic components of the RIME engine have been built for other applications. However, they have not been assembled as a high-power boost-phase propulsion system.

The Ayak concept being studied in Russia is an interesting version of using MHD for performance improvement.<sup>19</sup> Ramjets have substantially better performance than scramjets, but are limited by velocity. When hypersonic air is slowed to subsonic speeds for combustion in a ramjet, the energy in the compressed air is so high that combustion may not be able to occur. Scramjets allow the flow to remain at a supersonic level during combustion. The Ayak concept uses MHD to extract electrical energy from the kinetic energy of the incoming air, slowing it down for efficient ramjet operations. The electrical energy is then used to further accelerate the ramjet exhaust using MHD. This concept was presented in Munich in 1993 to the Fifth International Conference on Aerospacecraft and Hypersonic Technology.

Kelly has a concept which uses this same principle, but in reverse.<sup>20</sup> At subsonic or low supersonic speeds, ramjets do not have enough compression from the kinetic energy of the air flow to operate efficiently. Turbojets extract some energy from the jet exhaust to drive a compressor to improve efficiency. The Kelly concept uses MHD to extract energy from the exhaust and then applies this energy, via MHD, to compress the incoming air—a turbojet without the turbine.

#### Conceptual RIME Vehicle Sizing Analysis

A top-level vehicle sizing analysis was performed assuming a conical vehicle as shown in Fig. 13. Modular RIME engines are wrapped around the vehicle near the cone base. A 150-klb thrust  $\text{lox}/\text{H}_2$  engine was estimated to weigh 2,183 lb by linear scaling between existing engines, and was assumed to have an  $I_{sp} = 425$  s, between sea level and vacuum performance. The mass of the MHD

generator was obtained by scaling from the extensive "100-MW MHD generator system" design data developed by STD, Inc., to a 1-GW device required for our application. The design uses no superconducting technology.

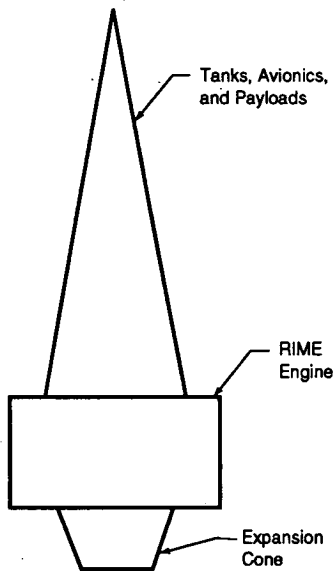


Fig. 13. RIME vehicle concept.

From MHD textbooks, power can be shown to scale with the square of the flow velocity ( $u^2$ ) and with the square of the magnetic field strength ( $B^2$ ).<sup>10</sup> An assumption is made that the MHD system weight scales linearly with the magnetic field,  $B$ . The rationale is that the magnet design drives the mass. Since one measure of field strength is amp turns, it follows that to increase strength by one amp turn, one simply adds a turn. This is a linear relationship. Conventional MHD system designers explain that their system mass usually scales with the square of  $B$  because of the additional structure required to hold the magnetic coils into a complex shape. To minimize the mass of the flight system, one should probably use a magnet design that takes advantage of the natural shape the magnet would tend to form. Nevertheless, the assumption here is that MHD system mass is linear with  $B$ . Conversations with MHD system designers indicate that accelerators are usually a little lighter in weight than generators. So, another assumption here is that the accelerator (including the ducts) and ionizer mass combined is the same as the generator.

From the earlier analysis and Fig. 10, a bypass ratio of 30 was selected giving a thrust augmentation ratio of 3.5, providing a total thrust of 525 klb, ignoring the effects of sea level pressure. A complete system design must account

for this and many other details. Using the data and scaling factors above yield the following:

#### Weight Results

- engine	2,183 lb
- generator	47,238 lb
- accelerator + ionizer	47,238 lb
- structure, avionics, tanks	50,000 lb
- propellant	300,000 lb
total	446,659 lb

This vehicle has a thrust-to-mass ratio of 1.175, so it may be able to get off the ground. The propellant mass fraction is  $f = 0.672$ . From the earlier analysis, this vehicle was shown to have marginal capability to reach orbit. Some additional capacity must be incorporated to ensure a landing capability. Significant performance improvements can be obtained by utilizing additional technologies that are currently available.

#### Avenues for RIME Enhancement

The mass of the magnets may be reduced by using superconducting magnet technology.<sup>17</sup> Since the fuel is liquid hydrogen, there is an ample supply of cryogen. If the mass of the MHD system could be reduced by a factor of 2, the payload to orbit goes from zero to 50,000 lb. For a half-million pound SSTO vehicle, this is impressive.

It may be possible to eliminate the ducts for the accelerator, reducing the vehicle mass and perhaps extending the bypass ratio above 30. This perhaps could be accomplished by creating external magnetic and electric fields such as the scalloped fields shown in Fig. 14.

The amount of required onboard oxidizer can perhaps be reduced by driving the generator with a ramjet, or perhaps an ejector, rather than a rocket. A rocket mode is, of course, still required since a space vehicle will eventually run out of atmosphere.

Increasing the diameter of the vehicle has both advantages and disadvantages. It would permit interaction with a larger amount of air, and may permit use of ground effects during takeoff and landing. At hypersonic velocities, the shock problem becomes significant. If a way can be found to manipulate the shocks, the ionization problem may be solved. Interacting shocks have developed temperatures of 5,000 °F, more than adequate to ionize air.

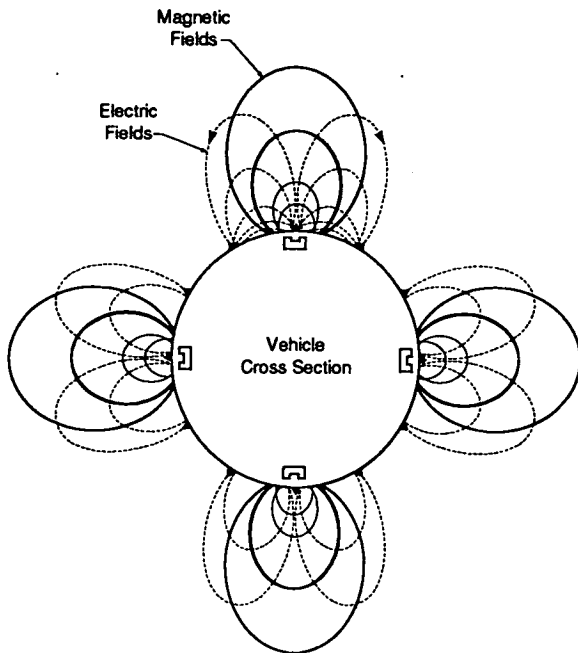


Fig. 14. Unducted RIME magnetic and electric field pattern.

#### Next Steps

Currently, there is no funded activity under way on RIME or MHD thrust augmentation. Should the means become available to pursue this concept further the following recommendations are offered.

- Develop some simple laboratory tests to demonstrate that air/MHD thrust augmentation is achievable.
- Acquire or develop MHD code to model the RIME engine concept.
- Acquire or develop CFD code to model the engine performance and characteristics.
- Conduct a vehicle systems analysis to understand how a RIME vehicle could be designed and operated. Identify and initiate system tests needed to demonstrate flight type component and system feasibility and design parameters.
- Develop and implement a technology development plan.

#### Conclusion

Technology exists to build an MHD thrust augmentation system for the atmospheric boost phase of an SSTO vehicle. Modest improvements in

technology will provide a system that far surpasses the performance of competing concepts for Earth-to-orbit transportation. A day will come when this is the way it is done, and the sooner the better.

#### References

1. Harper, R.E., and Zimmerman, J.H.: "An Investigation of Rocket Engine Thrust Augmentation With a Nozzle-Ejector System." AEDC-TDR-62-42, March 1962.
2. Evans, J.R., and Wolff, H.E.: "Performance of a Rocket Engine/Nozzle Ejector (RENE) Model Rocket Cluster." AEDC-TDR-64-155, July 1964.
3. "Experimental and Theoretical Investigations of the Rocket Engine-Nozzle Ejector (RENE) Propulsion System," Technical Report No. AFRPL-TR-65-66, April 1995.
4. Porter, J.L., and Squyers, R.A.: "An Overview of Ejector Theory." AIAA-81-1678, Aircraft Systems and Technology Conference, Dayton, Ohio, August 11-13, 1981.
5. Stroup, K.E., and Atkins, T.E.: "Supercharged Ejector Ramjet Subscale Feasibility Test Program." Report No. 20436, September 1968, The Marquardt Corporation, Van Nuys, CA.
6. Esher, W., and Czysz, P.: "Rocket-Based Combined-Cycle Powered Spaceliner Concept." IAF-93-S.4.478, 44th Congress of the International Astronautical Federation, October 16-22, 1993, Graz, Austria.
7. Siebenhar, A., Bulman, M.J., Sasso, S.E., and Schnackel, J.A.: "Strutjet-Powered Reusable Launch Vehicles." PRA-SA-ASO-NASA/Hqs./Martin Marietta, August 30, 1994, Presented at the Sixth Annual Propulsion Symposium, Cleveland, OH, September 13-14, 1994.
8. Rosa, R.J.: "Magnetohydrodynamic Energy Conversion." Hemisphere Publishing Co., Washington, DC, 1987.
9. Maxwell, C.D., and Demetriades, S.T.: "Initial Tests of a Lightweight, Self Excited MHD Power Generator." Presented at the 23rd Symposium on the Engineering Aspects of Magnetohydrodynamics, June 1985.

10. Maxwell, C.D., and Demetriades, S.T.: "Feasibility Assessment for Space-Based Multi-Megawatt MHD System: Preliminary Conceptual Design." STD Research Corporation Report STDR-87-9(J) prepared under contract DE-AC22-87PC79664, February 1988.
11. Maxwell, C.D., and Demetriades, S.T.: "Tests of a Portable Multi-Megawatt MHD Power Generator." Presented at the 28th Symposium on the Engineering Aspects of Magnetohydrodynamics, June 1990.
12. Grabowsky, W.R., Durran, D.A., and Mirels, H.: "Performance of a 500-kJ MHD Wind Tunnel." Aerospace report No. TR-0158(3240-10)-10, AF No. SAMSO-TR-68-222, March 1968.
13. Whitehead, G.L., Christensen, L.S., and Felderman, E.J.: "MHD Performance Demonstration Experiment—Final Report." Calspan Field Services, Inc., AEDC Division, DE-AI22-78ET11417-20.
14. Simmons, G., Nelson, G., Hiers, R., and Western, A.: "An Unseeded Air MHD Accelerator Concept for High Mach Number Hypersonic Propulsion." AIAA-89-2535, AIAA/ASME/SAE/ASEE 25th Joint Propulsion Conference, Monterey, CA, July 10-12, 1989.
15. Schultz, R.J., Chapman, J.N., and Rhodes, R.P.: "MHD Augmented Chemical Rocket Propulsion for Space Applications." The University of Tennessee Space Institute, AIAA-92-3001, 23rd Plasmadynamics and Lasers Conference, Nashville, TN, July 6-8, 1992.
16. Hingorani, N.G., and Stahlkopf, K.E.: "High-Power Electronics." *Scientific American*, vol. 269, Issue 5, November 1993, p. 78.
17. Boebinger, G., Passner, A., and Bevk, J.: "Building World-Record Magnets." *Scientific American*, June 1995, p. 58.
18. Crawford, R.A., Chapman, J.N., and Rhodes, R.P.: "Potential Application of Magnetohydrodynamic Acceleration to Hypersonic Environmental Testing." AEDC-TR-90-6, The University of Tennessee Space Institute, August 1990.
19. Novichkov, N.: "Russia in the Forefront of Aerospace Technology." *Aerospace Industry*, 1994, p. 68.
20. Kelly, M.S.: "An Open 'Brayton-Cycle' Engine for Operation at Hypersonic Speed." Internal report of Kelly Space and Technology, Inc., San Bernardino, CA, December, 1994.